JOURNAL OF MECHANICAL ENGINEERING AND SCIENCES (JMES)
ISSN: 2289-4659 e-ISSN: 2231-8380
VOL. 16, ISSUE 1, 8770 – 8787
DOI: https://doi.org/10.15282/jmes.16.1.2022.10.0693

ORIGINAL ARTICLE

Spacer effects on thermal-hydraulic performance of fluid flow at supercritical pressure in annular channel - CFD methodology

S.K. Dhurandhar[1*], S.L. Sinha[1] and S.K. Verma[2]

[1] Mechanical Engineering Department, National Institute of Technology Raipur, Raipur (C.G)-492010, India
Phone: +919300270626
[2] Cryopump and Pellet Injector Division and Advanced Computer Simulation Group, Institute for Plasma Research, Gandhinagar-382428, Gujarat, India

ABSTRACT – Spacer is a vital component in assembly of nuclear fuel rod bundles. It is used to support and maintain suitable distance between the rods in assembly of nuclear fuel bundle. Spacer promotes the local heat transfer in downstream to the spacer in rod bundle. The objective of present work is to analyse the spacer effects on thermal and hydraulic performance of R-134a at supercritical condition of pressure 4.5 MPa in an annular flow. A Computational Fluid Dynamics (CFD) code ANSYS Fluent has been used for present numerical analysis and SST (Shear Stress Transport) k-ω turbulence model was considered for turbulence flow analysis. Numerical analysis was carried out in an annular channel of 6 mm hydraulic diameter with spacer, located at middle of channel. Hydraulic and thermal performance due to the spacer have been investigated for three different mass flow rates (0.33175, 0.41469 and 0.53909 kg/s) and three different heat fluxes (60, 100 and 160 kW/m^2). Two blockage ratios of 0.3 and 0.38 have been used in present analysis. Due to the presence of spacer as flow obstruction, it is observed that at spacer location, velocity increased significantly and subsequent decrease in pressure. Also; it is noticed that the wall temperature is decreased and corresponding coefficient of heat transfer enhanced significantly at the location of spacer in annular channel. The observed value of ratio of Nusselt number for the case of spacer and without spacer (Nu/Nu*) shows better agreement with correlations data for flow obstacle at Re=97000.

ARTICLE HISTORY
Received: 16th Dec. 2020
Revised: 28th Dec. 2021
Accepted: 05th Jan. 2022

KEYWORDS
Heat transfer performance; flow characteristic; spacer; numerical simulation; supercritical pressure; annulus flow

INTRODUCTION

The analysis of thermal and hydraulic performance is a vital field for optimal design of spacers which are used with fuel rods in the core of nuclear reactor. Spacer is utilized as support for the rods in assembly of nuclear rod bundle, it reduces vibration between fuel rods and maintains required gap between the nuclear fuel rods. Spacer with fuel rod also enhances the rate of heat transfer due to the increased rate of mixing of coolant between sub channels which improves turbulence of flow. The flow direction of coolant is axially vertical in the assembly of nuclear fuel rods. Coolant is used to reduce the cladding temperature of fuel rod and to remove the heat from the surface of fuel rod. The flow of coolant in nuclear fuel rod with spacer is having complex structure and distribution in between fuel rods and hence the investigation of thermal distribution and hydraulic behaviour is a crucial part in the assembly of nuclear fuel rods. SCWR (supercritical pressure water cooled reactor) concept has been considered in development of the nuclear reactors for Generation-IV. SCWR has benefits of simple system, compactness and high thermal efficiency.

Analysis of spacer effects on thermal and hydraulic performance is an essential part in the view of thermal-hydraulic design of nuclear fuel rod assembly with spacer. Several experimental and computational investigations have been carried out to analyse the effects of spacer on heat transfer characteristics and flow behaviour at supercritical and subcritical pressures. Krall and Sparrow [1] experimentally observed the separated flow effect (which is due to orifices used as flow obstructions) on heat transfer. The working fluid used was water. They analysed the rate of heat transfer in heated tube with blockage ratios (BR) of 0.55, 0.75, 0.89 and 0.937. Blockage ratio can be defined as:

$$Blockage\ ratio\ (BR) = \frac{\text{Obstructed cross section area}}{\text{Unobstructed cross section area of the fluid domain}}$$

Koram and Sparrow [2] worked experimentally on heat transfer analysis of flow of water in circular tube with orifice plate used as flow obstruction. Three blockage ratios, 0.25, 0.5 and 0.75 were used for investigation. The analysis had been carried out for the Reynolds numbers of 11000, 15000, 25000, 40000 and 60000. Zhu et al. [3] investigated numerically the effect of standard spacer grid and spacer grid with split vanes on performance of heat transfer at supercritical pressure 25MPa of water in bundle of rod. They found that the presence of standard spacer grid and spacer grid with split vanes affect the rate of heat transfer. At spacer grid location, the rate of heat transfer found to be increased and in downstream locations, it decreased. Xiao et al. [4] numerically performed to analyse the effects of spacer on rate

*CORRESPONDING AUTHOR | S. K. Dhurandhar | ✉ satishdhurandhar@gmail.com

© The Authors 2022. Published by Penerbit UMP. This is an open access article under the CC BY license.

of heat transfer in an annular channel. They used supercritical R-134a as working fluid and found that in the spacer region local heat transfer coefficient improved significantly and in downstream, the rate of heat transfer reduced along with axial distance. Eter et al. [5] worked experimentally for the investigation on performance of heat transfer of supercritical CO_2 due to flow obstructions in tube. They observed that the largest improved effectiveness due to the obstructions can be seen at the larger enthalpies in liquid like region. Tanase and Groeneveld [6] experimentally investigated the influence of obstructions on heat transfer of R-134a in heated tube for the Reynolds number considered from 14200 to 97000. Three types of obstacles namely annular, blunt and rounded shaped with two blockage ratios 0.15 and 0.3 were used for analysis in circular heated tube. They developed a correlation for the ratio of Nusselt number (Nu/Nu^*) in terms of dimensionless axial distance and Reynolds number. Holloway et al. [7] conducted experiments for the measurement of heat transfer in 5 x 5 rod bundle for single phase water flow at Reynolds number 28000 and 42000. Two blockage ratios 0.14 and 0.2 were used for analysis of heat transfer and they proposed a correlation for Nusselt number (Nu/Nu^*) in terms of dimensionless axial distance and blockage ratio. Yao et al. [8] experimentally observed that the Nusselt number (Nu) is maximum for flow in nuclear fuel rod bundle at the flow obstruction or very near behind the obstruction and reduction in heat transfer enhancement is exponential after the spacer grid. Yao et al.[9] experimentally worked for analysis of heat transfer improvement and vortex shedding phenomena due to square shaped flow blockade used inside the channel of rectangular cross section. They conducted experiments for flow Reynolds number of 10500 and blockage ratio of 0.2. Doerffer et al. [10] experimentally investigated and observed that enhancement in transfer of heat is maximum at very near after the flow obstacle and reduction in enhancement of heat transfer is exponential in downstream after obstacle along with axial flow direction. They conducted experiments on ring type of flow obstruction with blockage ratios 0.178 and 0.3 and for Reynolds number of 39000 and 230000. Miller et al. [11] worked on 7 x 7 fuel rod bundle to analyse the heat transfer of steam (superheated) flow in downstream from spacer grid. They proposed a correlation for heat transfer with considering the blockage ratio effect, Reynolds number of flow and non-dimensional distance behind the grid spacer. Experimental analysis performed by Gu et al. [12] on 2 x 2 fuel rod bundle with wire wraps for single phase water at the condition of supercritical pressure. They observed that the wire wraps on fuel rod bundle increases the turbulence mixing and hence improves the heat transfer. An experimental observation conducted by Yang and Chung [13] with the help of laser Doppler velocimetry to predict the intensity of turbulence and velocity in downstream of spacer grid split vane. An investigation conducted through experiment by Caraghiaur et al. [14] for the turbulent flow on grid spacer of fuel rod bundle. They observed that the geometry configuration and location of spacer in fuel rod bundle cross section provide significant variations on flow structure and rate of heat transfer. Numerical and experimental investigations were carried out on performance of heat transfer by Wang et al. [15] for supercritical water. They considered the spiral shaped spacer as flow obstacle to predict the heat transfer in vertical annular channel. Numerical investigations were conducted on performance of heat transfer by Palko et al. [16], Jaromin and Anglart [17], and Cheng et al. [18] in vertical tube for upward flow of water at supercritical pressure. They reported that, SST k-ω turbulence model is more accurate for analysis of heat transfer at supercritical pressure. Xiao et al. [19] numerically investigated the deteriorated heat transfer (DHT) of R-134a flows at supercritical pressure in an annular channel with spacer. The deteriorated heat transfer mechanism was analyzed based on the turbulent kinetic energy and radial velocity distributions in downstream to the spacer. Also, other researchers worked with working fluid as R-134a flows at supercritical pressure to investigate the heat transfer characteristics and pressure drop in vertical circular tubes [20, 21]. Eze et al.[22] numerically studied the heat transfer deterioration of supercritical water due to vortex generators in upward flowing circular and annular channels. Spacer effects on heat transfer of water flows at supercritical pressure in an annular channel were analyzed by Hu and Gu [23] and discussed the enhancement in heat transfer downstream to the spacer. Numerical investigation were performed by Podia and Rao [24, 25] to study the heat and flow characteristics of supercritical pressure water in 2x2 rod bundle and validated the simulation results with experimental data. Leung et al. [26] worked on the assessment of CFD tools against with the experimental data of heat transfer at the pseudocritical region in the bundle subassemblies and discussed for the selection of the suitable turbulence model in the bundle assemblies. Wang et al. [27] provided a comprehensive review for both experimental and numerical studies on heat transfer to super-critical water (SCW) in rod bundles, annular channels and tubes. Numerical investigations were performed by many researchers [28–31] to study the effects of mixing vane spacer grids on heat and flow characteristics of water at subcritical pressures in rod bundles and they discussed about the selection of turbulence model for better prediction of flow phenomena inside the subchannel regions of rod bundles. Furthermore, direct numerical simulation (DNS) is an important method to analyze the heat transfer deterioration (HTD) of fluids at supercritical pressures in various channels [32, 33].

On the basis of above review, it can be concluded that presence of obstacle/spacer or mixing vanes grid spacer improve the turbulence mixing rate and enhance the heat transfer at the location of obstacle and close behind in downstream of the spacer. To predict the spacer effects on heat transfer at the condition of subcritical pressure several correlations were developed by researchers in terms of blockage ratio, dimensionless distance from the location of spacer and Reynolds number. Present investigation shows a CFD analysis for spacer effects on thermal and hydraulic performance of R-134a at supercritical condition of pressure of 4.5 MPa in an annular flow. A CFD code ANSYS Fluent has been used for numerical analysis and turbulent flow was modelled by using SST k-ω as turbulence model. In present study, spacers of two blockage ratio 0.3 and 0.38 have been used for analysis at supercritical pressure. Thermal-hydraulic performance analysis due to spacer has been investigated for three different mass flow rates (0.33175, 0.41469 and 0.53909 kg/s) and three different heat fluxes (60, 100 and 160 kW/m^2).The detailed analysis has been carried out with varying mass flow rates and heat fluxes for the spacer effects on thermal and hydraulic performance.

The presence of spacer provides advantages of enhanced heat transfer and flow characteristics in downstream to the spacer in an annular channel. Therefore, the present study will assist the understanding of enhanced thermal and hydraulic performance in a single rod channel with spacer. Also, the simulation data of this parametric study will assist the design and development of spacer in a single rod channel.

MATHEMATICAL MODEL

A three dimensional flow in annular channel has been considered for CFD analysis of spacer effects on thermal and hydraulic performance. Governing equations such as continuity, momentum and energy equations have been used in mathematical model for numerical investigation. Turbulence characteristics of flow have been simulated with using turbulence model as SST k-ω model.

Governing equations: The following governing equations have been used for simulation:

Continuity equation

$$\frac{\partial(u_i)}{\partial x_i} = 0 \tag{1}$$

Momentum equation

$$\frac{\partial(\mathrm{u_i})(\mathrm{u_j})}{\partial \mathrm{x_j}} = \mathrm{g_i} - \frac{1}{\rho}\frac{\partial(\mathrm{P})}{\partial \mathrm{x_i}} + \frac{1}{\rho}\frac{\partial}{\partial \mathrm{x_j}}\left[\mu\left(\frac{\partial(\mathrm{u_i})}{\partial \mathrm{x_j}} + \frac{\partial(\mathrm{u_j})}{\partial \mathrm{x_i}}\right) - \rho\overline{\mathrm{u_i}'\mathrm{u_j}'}\right] \tag{2}$$

Energy equation

$$\frac{\partial}{\partial x_i}[(u_i)(\rho E + P)] = \frac{\partial}{\partial x_i}\left[K\left(\frac{\partial T}{\partial x_i}\right) + (u_j)(\tau_{ij})\right] \tag{3}$$

Turbulence model- SST k-ω
Transport equation for k

$$\frac{\partial}{\partial \mathrm{t}}(\rho \mathrm{k}) + \frac{\partial}{\partial \mathrm{x_i}}(\rho \mathrm{k u_i}) = \frac{\partial}{\partial \mathrm{x_j}}\left(\Gamma_\mathrm{k}\frac{\partial \mathrm{k}}{\partial \mathrm{x_j}}\right) + \mathrm{G_k} - \mathrm{Y_k} + \mathrm{S_k} \tag{4}$$

Transport equation for ω

$$\frac{\partial}{\partial t}(\rho\omega) + \frac{\partial}{\partial x_i}(\rho\omega u_i) = \frac{\partial}{\partial x_j}\left(\Gamma_\omega\frac{\partial \omega}{\partial x_j}\right) + G_\omega - Y_\omega + D_\omega + S_\omega \tag{5}$$

The transport equations and values used for constants during simulation of SST k-ω turbulence model have been taken from ANSYS Fluent theory guide.

NUMERICAL APPROACH

Computational Domain and Boundary Conditions

The computational domain used in present study is illustrated in Figure 1. The fluid domain is a vertical flow annular channel of having 6 mm hydraulic diameter [4]. A spacer of length 10 mm is located at the middle of the channel to get analysed its effect on thermo-hydraulic characteristics of flow. Figure 2 shows the location of spacer in an annular channel. In present investigation, spacer of two blockage ratios 0.3 and 0.38 have been considered to analyse the hydraulic and thermal behaviour of flow due the presence of spacer. The length of annular channel is 1000 mm and spacer end location is at 500 mm from inlet of channel. Outer and inner diameters of the vertical flow annular channel are 25 and 19 mm respectively. In present study, the direction of fluid flow is upward vertical (i.e. in positive Y direction of computational domain coordinate system) in the annular channel. The detailed dimensions of computational domain are given in Table 1.

Table 1. Dimensions of computational domain

Parameters of computational domain	Value
Length of annular channel	1000 mm
Spacer end location from inlet	500 mm
Channel outside diameter	25 mm
Spacers length (located at mid of channel)	10 mm
Channel inside diameter	19 mm
Blockage ratio (BR) of spacers	0.3 and 0.38

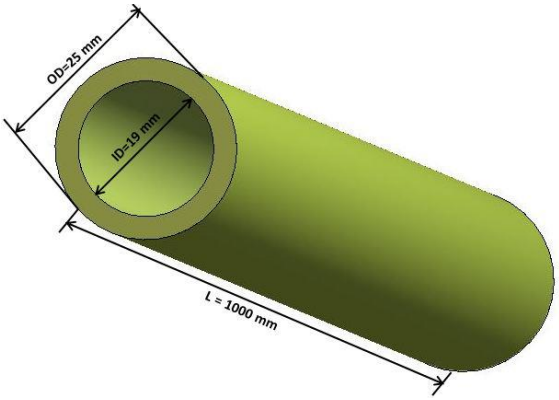

Figure 1. Computational domain - annular channel

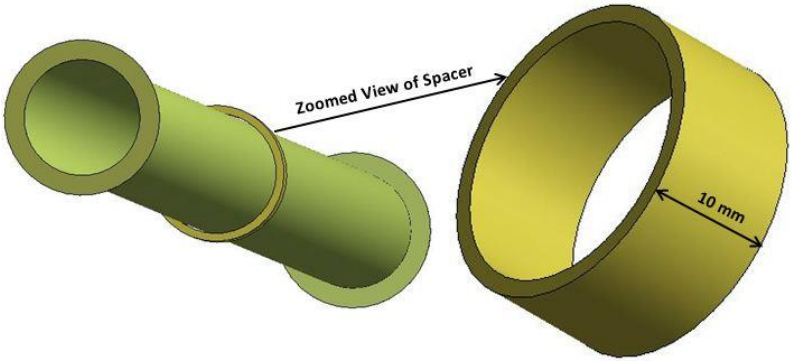

Figure 2. Location of spacer in annular channel

Boundary conditions used in present numerical analysis are shown in Figure 3. At inlet of fluid domain, the boundary condition set as mass flow rate, also fluid temperature, hydraulic diameter and turbulence intensity are given at inlet during simulation. Constant pressure boundary condition has been given at outlet of annular channel. Numerical investigation has been carried out for the effects of spacer on thermal and hydraulic characteristics under three different heat fluxes such as 60, 100 and 160 kW/m^2 and different mass flow rates of 0.33175, 0.41469 and 0.53909 kg/s. The properties of working fluid R-134a have been considered at 90^{0}C and supercritical pressure condition of 4.5MPa. The thermophysical properties of R134a at pressure 4.5 MPa have been taken from the National Institute of Standards and Technology (NIST) database which is shown in Figure 4. The boundary conditions used in present analysis are given in Table 2.

Table 2. Boundary conditions

Boundary	Boundary condition	Physical conditions
Inlet	Mass flow rate	0.33175, 0.41469 and 0.53909 kg/s
	Temperature	90 ^{0}C
Inner wall	Smooth and No-slip	Adiabatic wall
Outlet	Constant pressure	4.5 MPa
	Temperature	27 ^{0}C
Outer wall	Constant heat flux and no slip	60, 100 and 160 kW/m^2

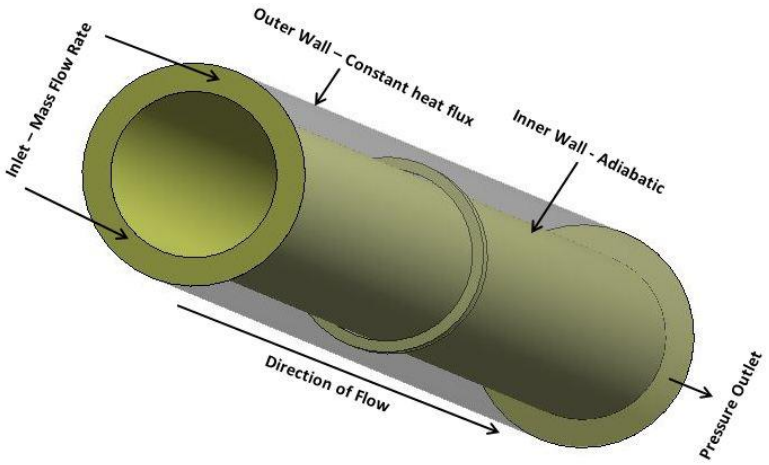

Figure 3. Boundary conditions used in annular channel

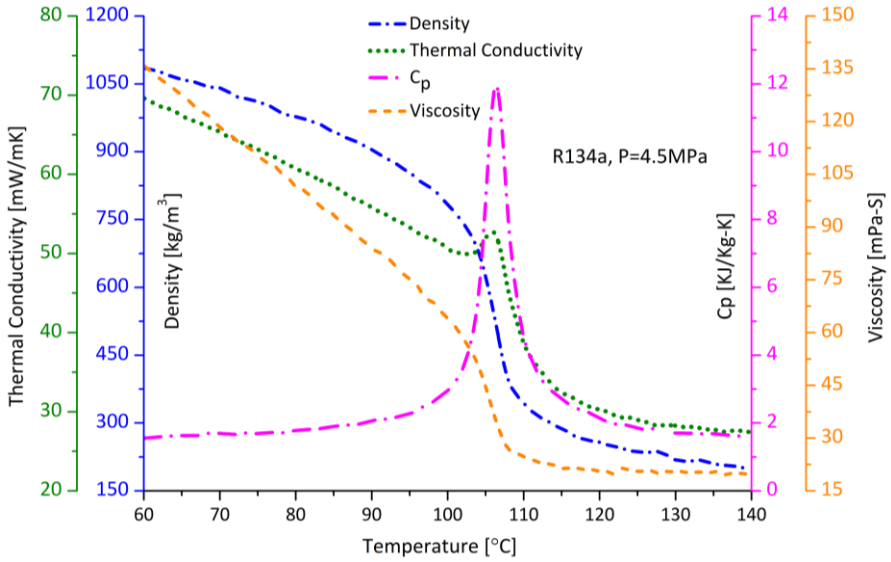

Figure 4. Thermophysical properties of R134a at supercritical pressure 4.5 MPa

Model Validation and Selection of Turbulence Model

Model validation has been performed with three turbulence models such as SST k-ω, Standard k-ε, and RNG k-ε in an annular channel without spacer against experimental data taken from Xiao et al. [19]. The geometry used for model validation is an upward flow annular channel without spacer having length; inner and outer diameters are 2.0, 0.019 and 0.025 m respectively. Validation has been performed for working fluid R134a and the parameters of mass flux as 500 kg/m^2s, heat flux as 55 kW/m^2 and pressure 4.5 MPa. Figure 5 shows the comparison of CFD results with experimental data (model validation) for the distribution of wall temperature versus enthalpy in an upward flow annular channel without spacer. It can be seen from the figure that the distribution of wall temperature against enthalpy for given flow conditions is the best predicted by the SST k-ω turbulence model as compared to Standard k-ε and RNG k-ε turbulence models. Based on this comparison, SST k-ω has been adopted as a turbulence model for further numerical simulations in the present study. Moreover, in the literature, it has been analysed by several researchers [16]–[18] that for heat transfer analysis of fluid flow at supercritical pressure, SST k-ω turbulence model is more accurate against other turbulence model.

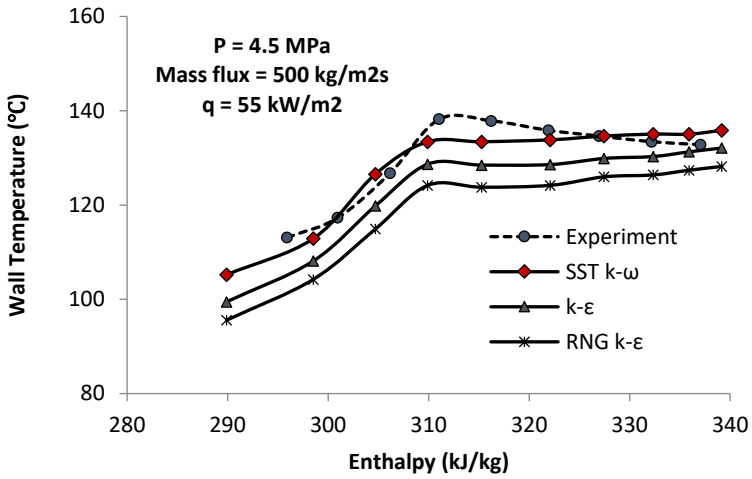

Figure 5. Model validation

Mesh System

The grid independence test has been carried out for the present investigation. Three systems of mesh have been used to conduct mesh independence test and for each system of mesh, near wall y^+ and mesh count are given in Table 3. For all three mesh systems, tangential velocity has been taken [as shown in Figure 6(a)] on the line drawn between inner wall and outer wall. The line drawn between inner wall and outer wall is at 400 mm from inlet of annular channel, which is shown in Figure 6(b). Based on comparison of result for tangential velocity versus radial distance from inner wall to outer wall of three cases, Case 2 from given Table 3 has been considered as baseline mesh system for further numerical investigation. Tetrahedron element type of mesh has been used for meshing of the geometry and surface mesh with tetrahedron element on inner wall and spacer is shown in Figure 7(a). Six prism layers have been created near wall to capture flow characteristics significantly close to wall. Volume mesh between inner and outer wall with prism layers is shown in Figure 7(b).

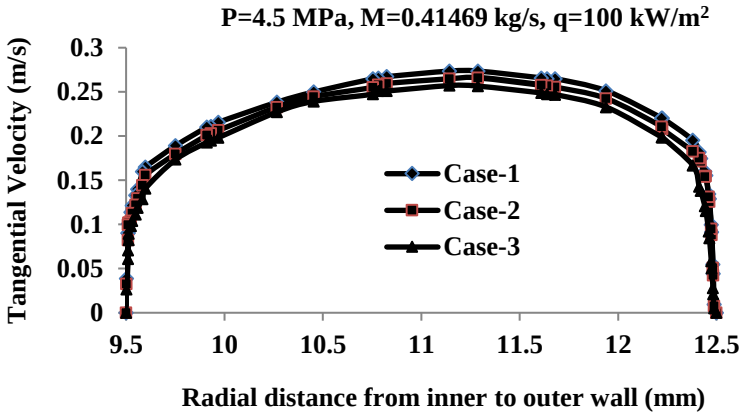

Figure 6. (a) Grid independency test

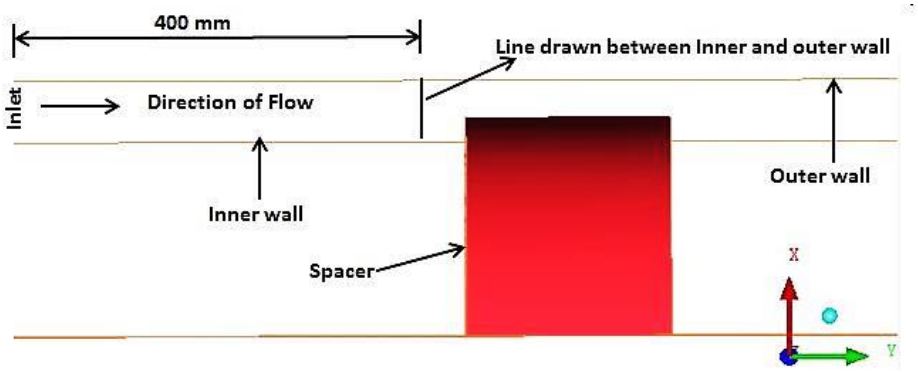

Figure 6. (b) Line drawn between inner wall and outer wall is at 400 mm from inlet of annular channel

Table 3. Mesh systems

Case	Mesh count	Minimum y^+ near wall
1	1.9 million	0.3
2	1.6 million	0.6
3	1.3 million	0.8

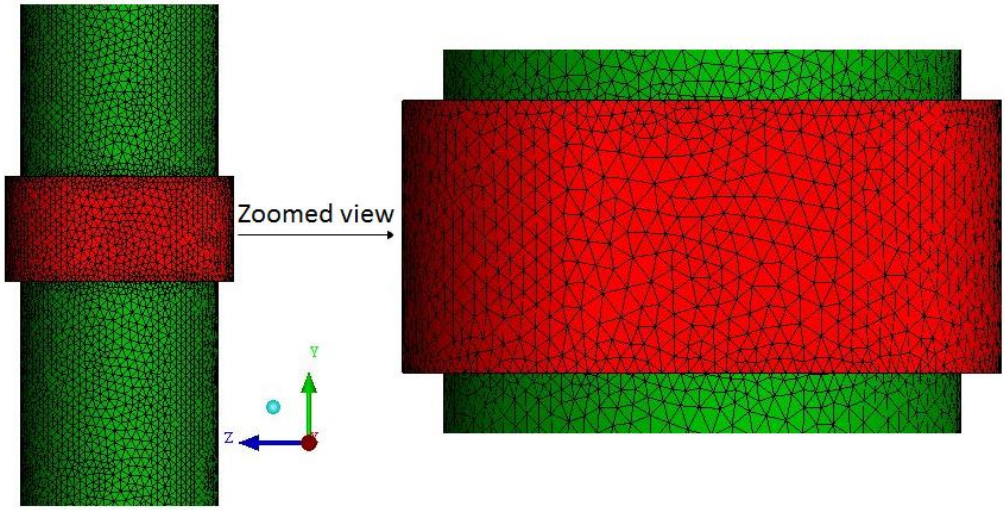

Figure 7. (a) Surface mesh of inner wall and Spacer

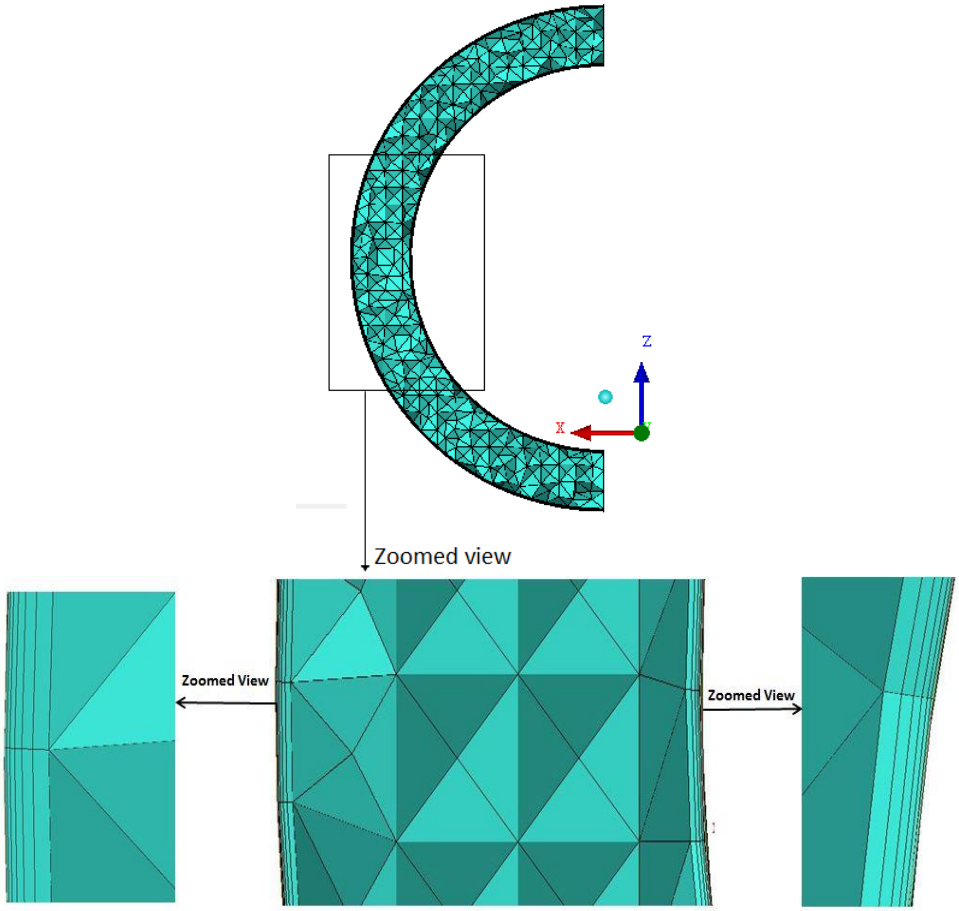

Figure 7. (b) Volume mesh between inner and outer wall

Solution Methodology

The SIMPLE algorithm has been implemented for the pressure-velocity coupling. Initially, a converged solution achieved with residual value of 10^{-6} by using first-order upwind discretization scheme for the momentum, turbulent kinetic energy, specific turbulence dissipation rate and energy equation. And then, the second-order upwind is set as discretization scheme for further simulation and the residual value of 10^{-4} achieved for the velocity components, turbulent kinetic energy, specific turbulence dissipation rate. These schemes along with the residual convergence criteria ensure the accuracy of the obtained results. To improve the solution convergence, the under-relaxation factors have been reduced for pressure and momentum from their initial values to 0.2 and 0.5 respectively. The effect of gravity is included for completeness of the computational model.

RESULTS AND DISCUSSION

Spacer Effects on Performance of Heat Transfer

The effects of spacer on heat transfer performance in an annular channel with blockage ratio 0.38 and with varying heat fluxes are shown in Figure 8 (a-c). Results shown in Figure 8 are obtained by taking constant system pressure as 4.5 MPa, constant mass flow rate as 0.41469 kg/s, blockage ratio as 0.38 and with varying heat fluxes as 60, 100 and 160 kW/m^2. The wall temperature, coefficient of heat transfer and ratio of coefficient of heat transfer with and without spacer (CHT/CHT*) are illustrated in Figure 8 (a), (b) and (c) respectively. X/D (Non-dimensional distance) is drawn on abscissa, where X is axial distance in flow direction and D represents as hydraulic diameter of the annular channel. Wall temperature is reduced at the spacer zone, around 4^0C, 8^0C and 12^0C for the heat fluxes 60,100 and 160 kW/m^2 respectively, which is shown in Figure 8 (a). It can also be seen from Figure 8 (a), that as heat flux increases, the corresponding wall temperature increases along the length. Figure 8 (b) represents result between coefficient of heat transfer at ordinate and non-dimensional distance (X/D) on abscissa, it shows that, significant enhancement in coefficient of heat transfer at the zone of spacer for all the three heat fluxes, which is because of the flow velocity improvement at location of spacer. Increased flow velocity in spacer zone is caused by reduced flow area, which is due to presence of spacer which acts as flow obstacle. It is also found that the coefficient of heat transfer increases within the zone of spacer as heat flux increases. The ratio of coefficient of heat transfer (CHT/CHT*) at spacer location is found to be about 1.65, 1.88 and 2.24 for the heat fluxes 60,100 and 160 kW/m^2 respectively, which is shown in Figure 8 (c). It can also be seen from Figure 8 (c) that, the effect of spacer in downstream annular flow is observed as the enhancement of ratio of coefficient of heat transfer (CHT/CHT*) up to about the non-dimensional distance X/D=30 for both the heat fluxes of 60 and 100 kW/m^2. The effect of spacer on ratio of coefficient of heat transfer (CHT/CHT*) is found in downstream flow up to the non-dimensional distance X/D = 40 for heat flux of 160 kW/m^{2}and then flow of fluid is become fully developed in the channel. The trend of distributions for the wall temperature, coefficient of heat transfer and ratio of coefficient of heat transfer (discussed in this section) are similar to the work accomplished for supercritical water in rod bundle with spacer grid [3].

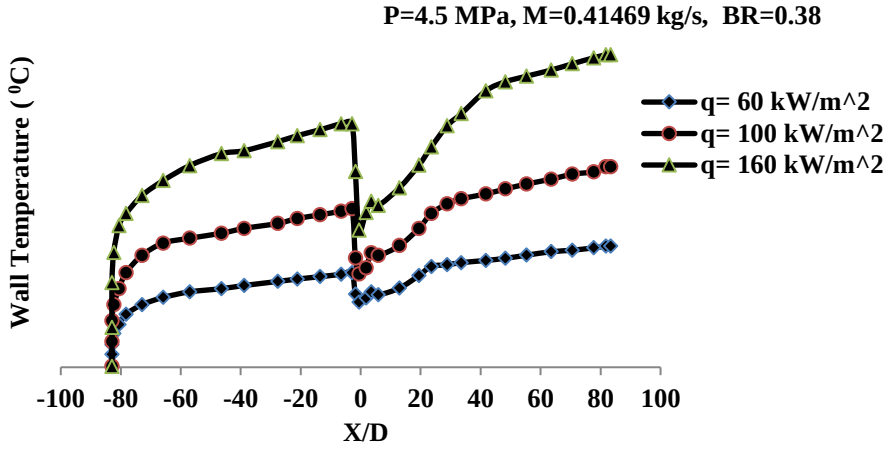

(a) Wall Temperature

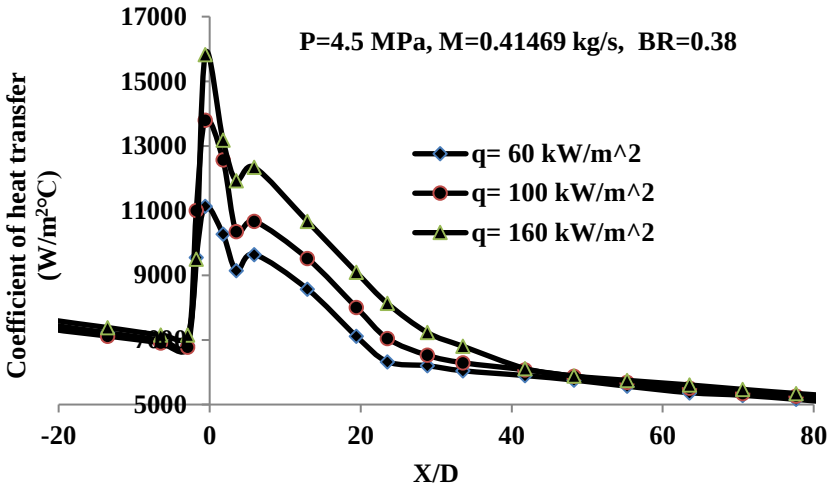

(b) Coefficient of heat transfer

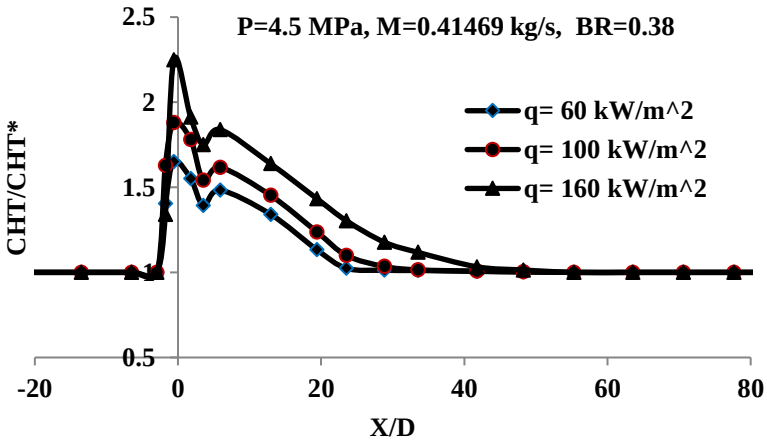

(c) Ratio of coefficient of heat transfer

Figure 8. (a-c) Spacer effects on heat transfer performance with varying heat flux

Figure 9 (a-c) represents the influences of spacer on the heat transfer performance in annular channel with varying mass flow rates. The results shown in Figure 9 are obtained by taking system constant pressure as 4.5MPa, constant heat flux as 100 kW/m^2, blockage ratio as 0.38, and for different mass flow rates 0.33175, 0.41469 and 0.53909 kg/s. The effect of spacer on wall temperature, coefficient of heat transfer and ratio of coefficient of heat transfer with and without spacer (CHT/CHT*) are shown in Figure 9 (a), (b) and (c) respectively.

It is clear from Figure 9(a) that, as mass flow rate increases, the corresponding wall temperature decreases due to increased flow velocity. Within the spacer region, the wall temperature reduced over 6^{0}C, 8^{0}C and 11.5^{0}C for the mass flow rates of 0.53909, 0.41469 and 0.33175 kg/s respectively. Figure 9 (b) shows result between coefficient of heat transfer and non-dimensional distance X/D, it can be seen in this figure that the corresponding coefficient of heat transfer improves with increase in mass flow rate and, also at the region of spacer, the increase in coefficient of heat transfer is significant which is due to increase in flow velocity at the spacer location. Figure 9 (c) shows that, as mass flow rate increases, corresponding ratio of coefficient of heat transfer (CHT/CHT*) increases and within spacer region, the enhancement is significant due to reduction in flow area. The maximum ratio of coefficient of heat transfer is found at spacer location which is about 1.8, 1.88 and 2.01 for the mass flow rates of 0.33175, 0.41469 and 0.53909 kg/s respectively. The effect of spacer in enhancement of ratio of coefficient of heat transfer is found in downstream to spacer up to about X/D=30 for both the mass flow rate of 0.33175 and 0.41469 kg/s, and for mass flow rate of 0.53909 kg/s, this effect is found up to about X/D=43 in downstream to the spacer.

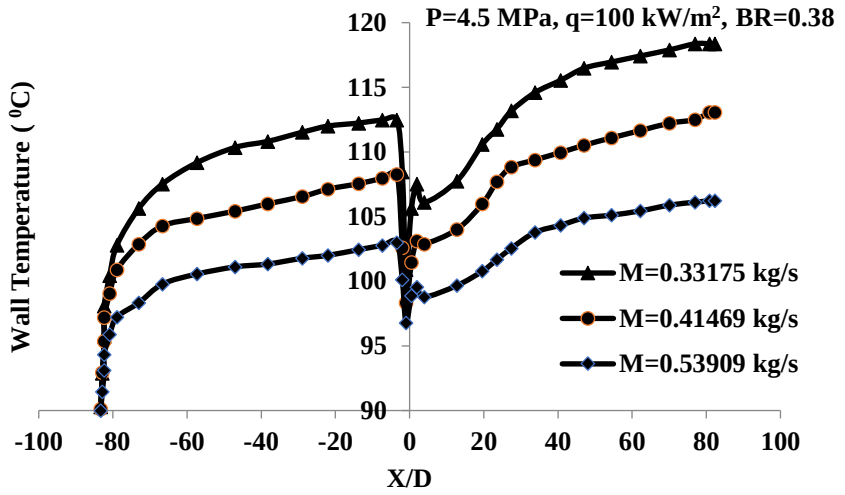

(a) Wall Temperature

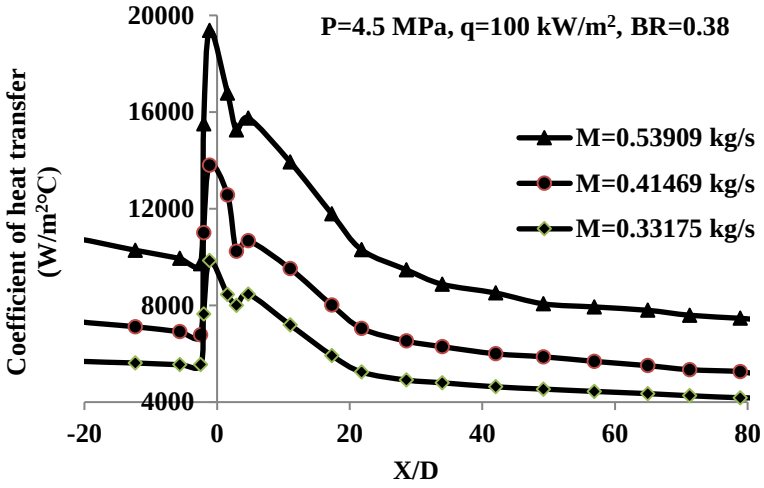

(b) Coefficient of heat transfer

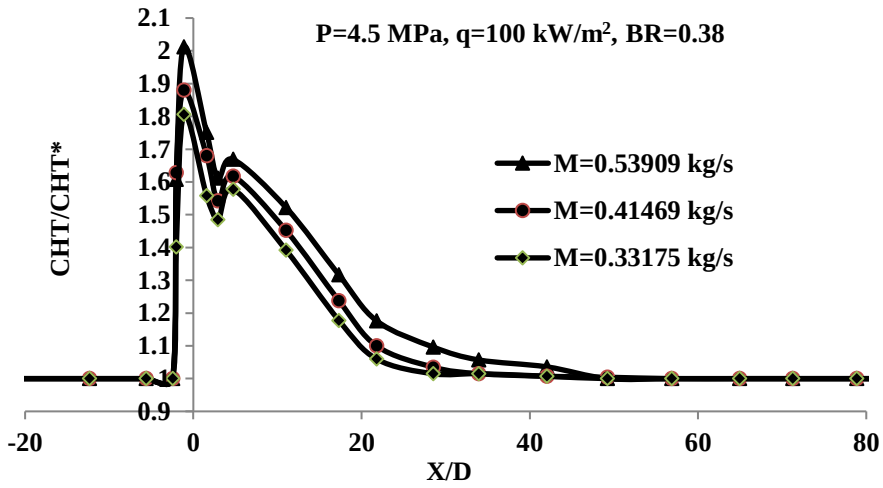

(c) Ratio of coefficient of heat transfer

Figure 9. (a-c) Spacer effects on heat transfer performance with varying mass flow rate

Figure 10 represents the temperature contour of the annular channel wall. The temperature contour is taken for the mass flow rate as 0.41469 kg/s, heat flux as 100 kW/m2, blockage ratio as 0.38 and constant system pressure as 4.5 MPa. The effect of spacer on wall temperature can be seen form the Figure 10. The wall temperature increases gradually prior to the spacer location and suddenly reduces at the spacer region in the flow direction. The magnitudes of wall temperature at just prior and immediate after to the spacer in the flow direction are about 381 K (108 ^{0}C) and 373 K (100 ^{0}C). Thus, the reduction in wall temperature within the spacer region is observed about 8 ^{0}C. As, the fluid (R134a) bulk temperature depends on the wall temperature, the fluid bulk temperature appears similar trend in the present study as wall temperature

of the channel. For Isobaric Properties of R134a, the supercritical phase starts at 101 ^{0}C for 4.5 MPa. The pseudocritical temperature is 106.3 ^{0}C of R134a for 4.5 MPa pressure. The wall temperature peak appears when the fluid bulk temperature is near to the pseudocritical temperature [19].

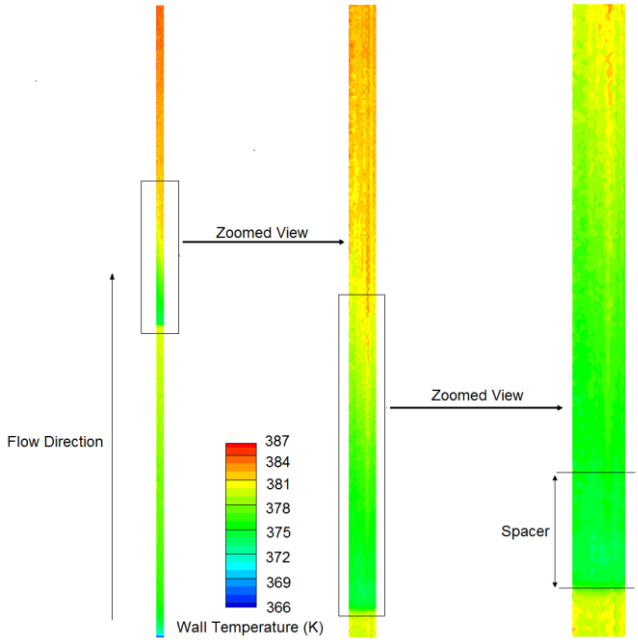

Figure 10. Temperature contour of the annular channel wall

Spacer Effects on Flow Characteristics

The effects of spacer on axial velocity profile and static pressure distribution along a line which is at 0.5 mm distance from outer wall of annular channel have been shown in Figure 11 and Figure 12 respectively. Results shown in Figure 11 and 12 are obtained by taking the blockage ratio as 0.38, heat flux as 100 kW/m2 and 4.5 MPa of system pressure with varying mass flow rates. The line drawn at 0.5 mm distance from outer wall in annular channel is shown in Figure 13.

It can be seen form Figure 11 that, the magnitude of axial velocity is higher for the higher mass flow rate. The axial velocity magnitude is maximum at the location of spacer in an annular channel which is because of the decreased area of flow. This decreased area of flow is caused by the spacer. The values of maximum axial velocity within the spacer region are about 3.3, 4.1 and 5.3 m/s for the mass flow rates of 0.33175, 0.41469 and 0.53909 kg/s respectively. Figure 12 illustrates the result between static pressure in Pascal and non-dimensional distance X/D. It shows that, as the value of mass flow rate increases, the value of corresponding static pressure also increases and there is significant reduction of pressure at the location of spacer which is due to reduced flow area. The values of pressure reduction within the spacer region are about 2.6, 6.1 and 9.5 kPa for the mass flow rates of 0.33175, 0.41469 and 0.53909 kg/s respectively.

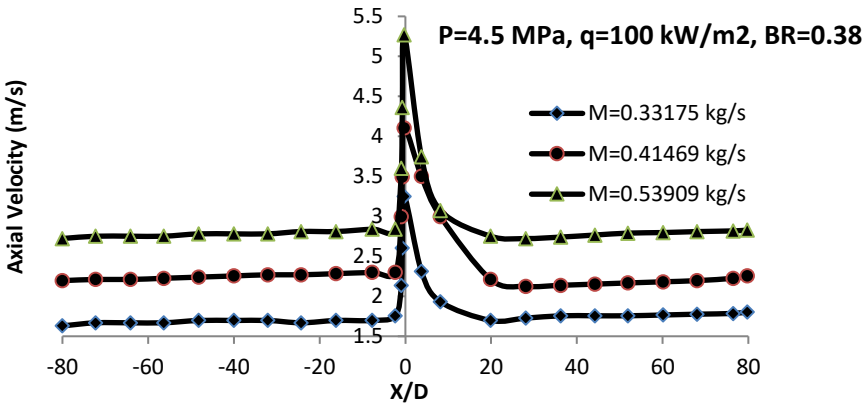

Figure 11. Axial velocity profile

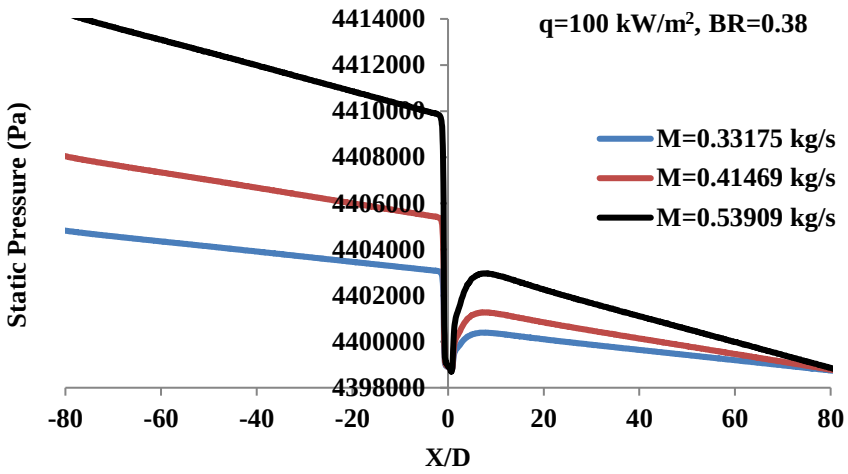

Figure 12. Static pressure distribution

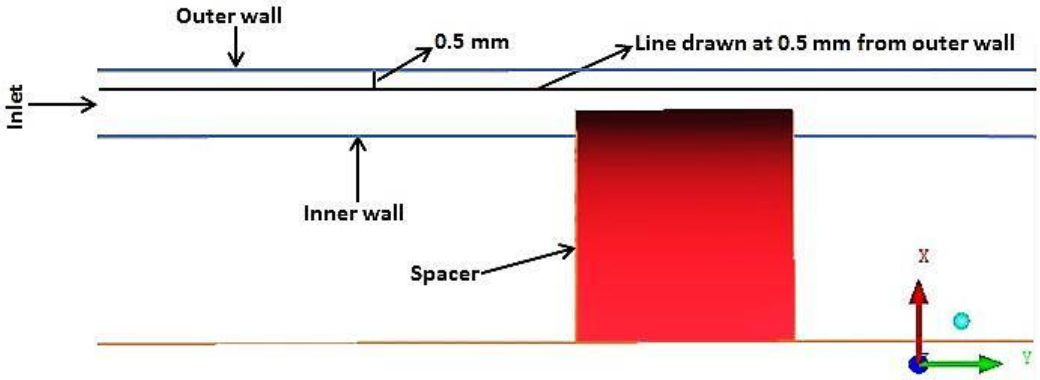

Figure 13. Line drawn at 0.5 mm distance from outer wall in an annular channel

Figure 14 represent the axial velocity contours on the location of spacer i.e. X/D=0 and other different axial locations in downstream direction after the location of spacer which are taken at X/D = 0.5, 1, 2, 5 and 30. These various axial locations taken are shown in Figure 14 (a), (b), (c), (d), (e) and (f) respectively. The axial velocity contours shown in Figure 14 are obtained by taking mass flow rate as 0.41469 kg/s, heat flux as 100 kW/m^2, blockage ratio as 0.38 and constant system pressure as 4.5 MPa. Figure 14 (a) shows that the axial velocity is maximum about 4.5 m/s near to the outer wall at the location of spacer i.e. X/D =0. This maximum axial velocity is observed near to outer wall because of minimum flow area occurred due to presence of spacer in annular channel. Similarly, the maximum velocity is observed near to the outer wall which is about 3.6 m/s at X/D=0.5. It can also be seen for the locations after spacer in downstream like at X/D= 1, 2 and 5, the axial velocity decreases but for all the locations velocity is maximum close to the wall. Figure 14 (f) shows that, the spacer effect in downstream at X/D=30 is almost negligible, maximum velocity which is about 2.6 m/s has been found at centre line of annular channel and in downstream to X/D =30, the flow is turn into fully developed in the channel.

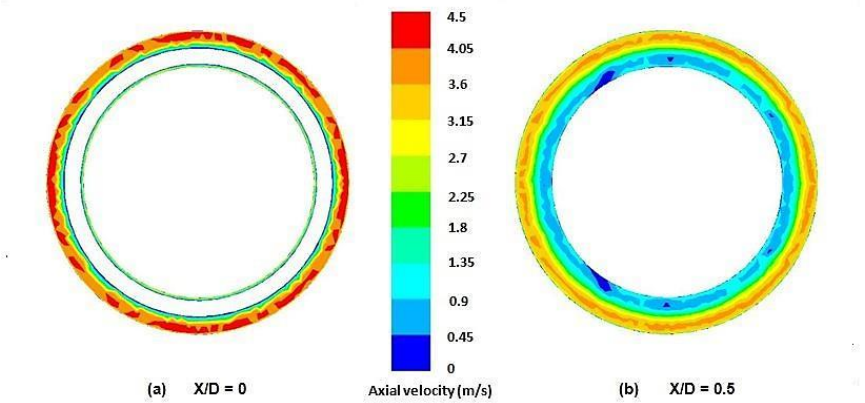

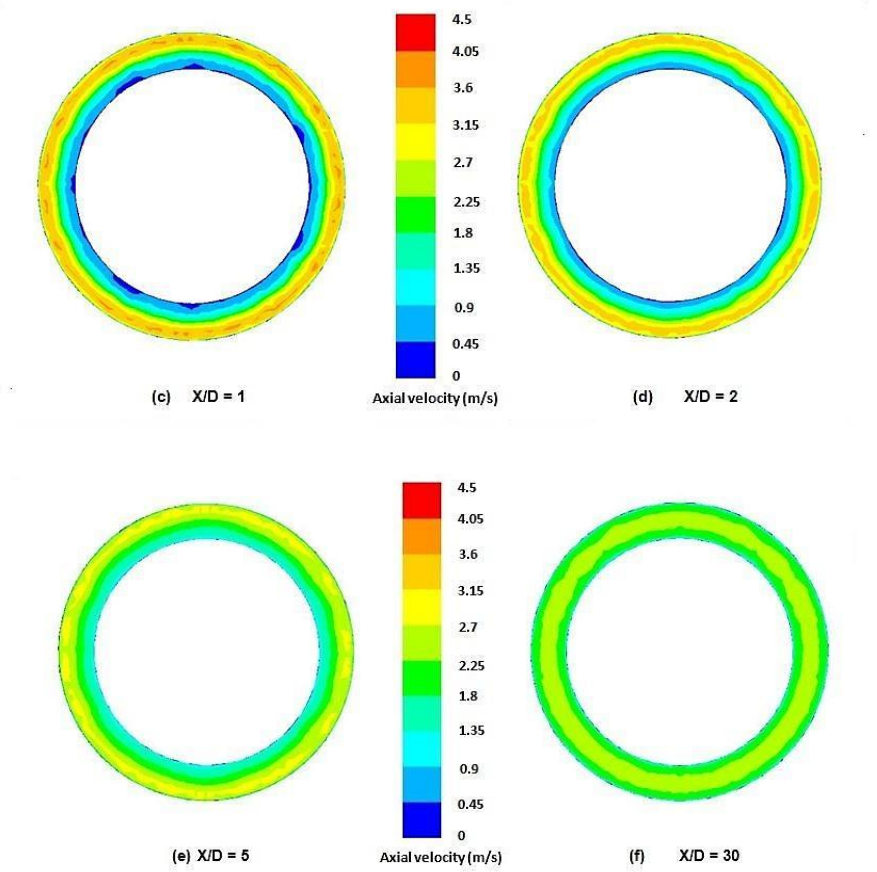

Figure 14. Axial velocity contours at the spacer (X/D=0) and different axial locations (X/D=0.5, 1, 2, 5 and 30) in downstream flow after spacer

Figure 15 shows the radial distribution of turbulent kinetic energy at X/D = 2, 5, and 15 in downstream after the location of spacer. The magnitude of turbulence kinetic energy is observed to be maximum at X/D=2 as it is near to the spacer in downstream. In downstream to spacer, for X/D =5 and 15, the magnitude of turbulent kinetic energy decreases as compared to X/D=2. It can also be seen from Figure 15 that, again near to the outer wall region the turbulent kinetic energy increases because of minimum flow area occurred due to presence of spacer [19].

Figure 16 shows the comparison of radial distribution of turbulent kinetic energy for two blockage ratios of 0.3 and 0.38. This comparison has been made at the locations X/D =2 and X/D = 5 in downstream to the spacer. The comparison of turbulent kinetic energy made for the flow condition of mass flow rate as 0.41469 kg/s, heat flux as 100 kW/m^2 and pressure as 4.5 MPa. It can be observed from Figure 16 that, for the same location in downstream to spacer, the magnitude of turbulent kinetic energy taken in radial direction is higher for the higher value of blockage ratio as the large blockage ratio gives large reduction of flow area in fluid domain. In comparison, it has also been found that turbulent kinetic energy again increases near the outer wall due to spacer effect which reduces the flow area [19].

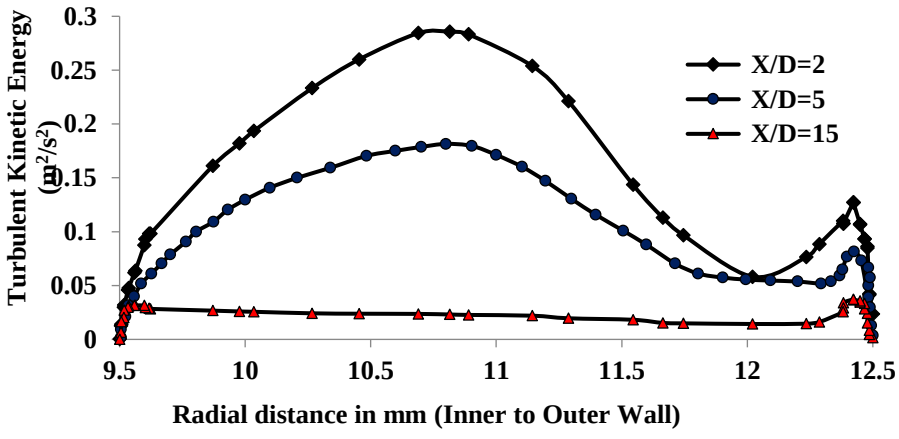

Figure 15. Turbulent kinetic energy profile (For M= 0.41469 kg/s, P=4.5 MPa, q=100 kW/m2 and BR=0.38)

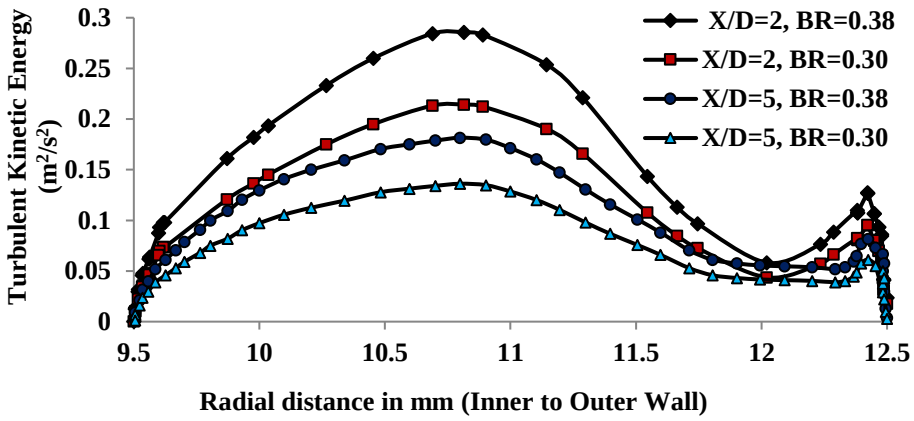

Figure 16. Comparison of turbulent kinetic energy

Comparison of CFD Result with Correlations

Figure 17 illustrates the comparison of CFD result with the correlations proposed for the flow obstacle (spacer) by many researchers. Correlations taken for comparison with CFD result have been developed for single phase working fluid at subcritical pressures and used to predict the effect of flow obstacle (spacer) on heat transfer such as Nusselt number ratio (Nu/Nu^*). These correlations for the ratio of Nusselt number (Nu/Nu^*) are established in terms of non-dimensional axial distance (X/D), Reynolds number (Re) and blockage ratio (ε), are given below:

On the basis of experimental data, a correlation proposed by Tanase and Groeneveld [6] for flow obstacles in heated vertical tube with working fluid R-134, is given as

$$\frac{Nu}{Nu^*} = 1 + 3.58 \times 10^{-5} Re\varepsilon^{\{0.47\ln(Re)-3.32\}} e^{-0.13(\frac{X}{D_h})} \quad (6)$$

Miller et al. [11] suggested a correlation based on experimental measurement for flow obstruction in 7 x 7 fuel rod bundle with working fluid superheated steam, is given as

$$\frac{Nu}{Nu^*} = 1 + 465.4Re^{-0.5}\varepsilon^2 e^{-7.31\times10^{-6}Re^{1.15}(\frac{X}{D_h})} \quad (7)$$

Holloway et al. [7] developed a correlation by experimental data for flow obstruction in 5 x 5 rod bundle with working fluid water, is given as

$$\frac{Nu}{Nu^*} = 1 + 6.5\varepsilon^2 e^{-0.8(\frac{X}{D_h})} \quad (8)$$

Yao et al. [8] developed a correlation for flow obstacle in rod bundle with working fluid water, is given as

$$\frac{Nu}{Nu^*} = 1 + 5.55\varepsilon^2 e^{-0.13(\frac{X}{D_h})} \quad (9)$$

Accurate correlation has not been found to predict the effect of flow obstacle on the performance of heat transfer [such as ratio of Nusselt number (Nu/Nu*)] for fluid flow at supercritical pressure, hence the present CFD result has been compared (Figure 17) with the above mentioned correlations [Eq. (6) to (9)] which have been developed for condition of subcritical pressures. Figure 17 shows the result between Nusselt number ratio (Nu/Nu*) and non-dimensional distance (X/D) after spacer. Present CFD result used for comparison is obtained by considering the heat flux as 60 kW/m^2, blockage ratio as 0.3 and Reynolds number of 97000. The result shows that, trend of present CFD result is similar to the correlations but it over predicts the of Nusselt number for the case of spacer and without spacer (Nu/Nu*). The supercritical pressure condition of fluid flow might be the reason of over prediction of ratio of Nusselt number (Nu/Nu*) as compared to the correlations data. The percentage deviations of the present CFD result with previous published correlations data has been given in Table 4.

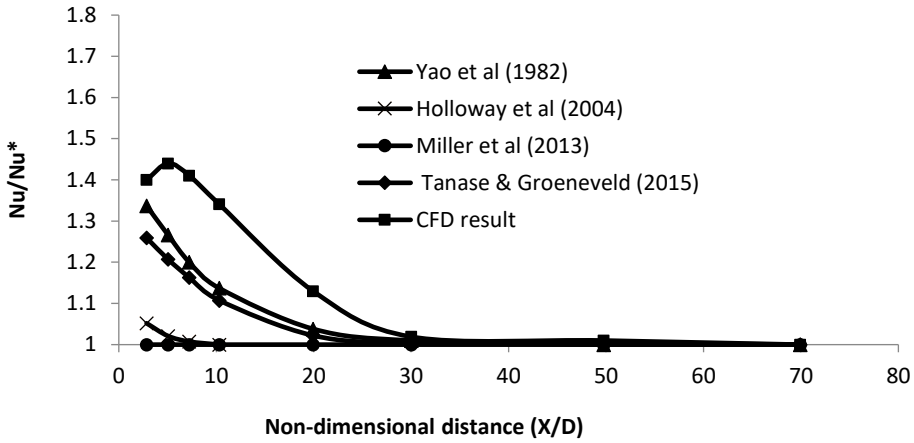

Figure 17. Comparison of CFD result with correlations (For BR=0.3 and Re=97000)

Table 4. Percentage deviations of the CFD result with correlations data

Present Work	Percentage deviations with correlations data			
	Yao et al. (1982)	Holloway et al. (2004)	Millet et al. (2013)	Tanase and Groeneveld (2015)
CFD result	7 %	14.1 %	15 %	9 %

CONCLUSIONS

The present investigation shows a CFD analysis for spacer effects on thermal and hydraulic performance of R-134a at supercritical pressure in an annular flow. A CFD code ANSYS Fluent has been used for numerical analysis of R-134a at pressure of 4.5 MPa and SST k-ω has been used as turbulence model for turbulence simulation. In present study, spacers of two blockage ratio 0.3 and 0.38 have been used for analysis at supercritical pressure. The detailed analysis has been carried out with varying mass flow rates and heat fluxes for the spacer effects on thermal and hydraulic performance and the following conclusions have been drawn:

1) The effect of spacer in an annular channel shows that the temperature of wall has been reduced which provide the safety of the surface of fuel rod from high cladding temperature and the enhancement in corresponding coefficient of heat transfer is found significant in the spacer region.
2) At the location of spacer, the velocity magnitude is maximum due to reduced flow area occurred which is caused by the presence of spacer in an annular channel. The spacer effect in downstream to spacer at X/D=30 is almost negligible, maximum velocity which is about 2.6 m/s has been found at the centre line of annular channel at X/D=30 and in downstream to X/D =30, flow of fluid is turn into fully developed in the channel.
3) Higher the value of mass flow rate, the value of corresponding static pressure is higher and there is significant reduction of pressure at the location of spacer because of presence of spacer which reduces the flow area.
4) Comparison of CFD result with correlations for flow obstacle shows that, trend of present CFD result is similar to the correlations but it over predicts the ratio of Nusselt number for the case of spacer and without spacer (Nu/Nu*) at Re=97000.

ACKNOWLEDGMENTS

Authors acknowledge the co-operation and support extended by the authorities of National Institute of Technology Raipur for the present work.

NOMENCLATURE

BR	Blockage ratio
C_p	Specific heat (J/kg.K)
CFD	Computational Fluid Dynamics
CHT	Coefficient of heat transfer (W/m^2.K)
CHT*	Coefficient of heat transfer without spacer (W/m^2.K)
D	Hydraulic diameter (m)

D_ω	Cross- diffusion term
E	Total energy (J)
g	Gravitational acceleration (m/s^2)
G_k	Production of turbulent kinetic energy
G_ω	Production of specific turbulence dissipation rate
h	Enthalpy (kJ/kg)
ID	Inner diameter of annular channel (m)
K	Thermal conductivity (W/m.K)
k	Turbulence kinetic energy (m^2/s^2)
L	Length of fluid domain (m)
M	Mass flow rate (kg/s)
Nu	Nusselt number
Nu*	Nusselt number without spacer
OD	Outer diameter of annular channel (m)
P	Pressure (Pa)
q	Heat flux (kW/m^2)
Re	Reynolds number
S_k	source term of turbulent kinetic energy
S_ω	source term of specific turbulence dissipation rate
T_w	Wall temperature (^{0}c)
u	Velocity component in x-direction (m/s)
u_i	Velocity vector (m/s)
(u)	Ensemble average quantity
(u′)	Turbulent fluctuating quantity
x_i	Coordinate vector (m)
X/D	Non-dimensional distance
Y^+	Non-dimensional perpendicular distance from wall
Y_k	Dissipation of turbulent kinetic energy
Y_ω	Dissipation of specific turbulence dissipation rate

Greek Symbols

ω	Specific turbulence dissipation rate (m^2/s^3)
τ_{ij}	Reynolds stress tensor
Γ_k	Effective diffusivity of turbulent kinetic energy
Γ_ω	Effective diffusivity of specific turbulence dissipation rate

REFERENCES

[1] K. M. Krall and E. M. Sparrow, "Turbulent heat transfer in the separated, reattached, and redevelopment regions of a circular tube," *Journal of Heat Transfer*, vol. 88, no. 1, pp. 131–136, 1966, doi: 10.1115/1.3691456.

[2] K. K. Koram and E. M. Sparrow, "Turbulent heat transfer downstream of an unsymmetric blockage in a tube," *Journal of Heat Transfer*, vol. 100, no. 4, pp. 588–594, 1978, doi: 10.1115/1.3450861.

[3] X. Zhu, S. Morooka, and Y. Oka, "Numerical investigation of grid spacer effect on heat transfer of supercritical water flows in a tight rod bundle," *International Journal of Thermal Sciences*, vol. 76, pp. 245–257, 2014, doi: 10.1016/j.ijthermalsci.2013.10.003.

[4] Y. Xiao, J. Pan, and H. Gu, "Numerical investigation of spacer effects on heat transfer of supercritical fluid flow in an annular channel," *International Journal of Heat and Mass Transfer*, vol. 121, pp. 343–353, 2018, doi: 10.1016/j.ijheatmasstransfer.2018.01.030.

[5] A. Eter, D. Groeneveld, and S. Tavoularis, "Convective heat transfer in supercritical flows of CO2 in tubes with and without flow obstacles," *Nuclear Engineering and Design*, vol. 313, pp. 162–176, 2017, doi: 10.1016/j.nucengdes.2016.12.016.

[6] A. Tanase and D. C. Groeneveld, "An experimental investigation on the effects of flow obstacles on single phase heat transfer," *Nuclear Engineering and Design*, vol. 288, pp. 195–207, 2015, doi: 10.1016/j.nucengdes.2015.04.004.

[7] M. v Holloway, H. L. McClusky, D. E. Beasley, and M. E. Conner, "The effect of support grid features on local, single-phase heat transfer measurements in rod bundles," *Journal of Heat Transfer*, vol. 126, no. 1, pp. 43–53, 2004, doi: 10.1115/1.1643091.

[8] S. C. Yao, L. E. Hochreiter, and W. J. Leech, "Heat-transfer augmentation in rod bundles near grid spacers," *Journal of Heat Transfer*, vol. 104, no. 1, pp. 76–81, 1982, doi: 10.1115/1.3245071.

[9] M. Yao, M. Nakatani, and K. Suzuki, "Flow visualization and heat transfer experiments in a turbulent channel flow obstructed with an inserted square rod," *International Journal of Heat and Fluid Flow*, vol. 16, no. 5, pp. 389–397, 1995, doi: 10.1016/0142-727X(95)00047-T.

[10] S. Doerffer, D. C. Groeneveld, and J. R. Schenk, "Experimental study of the effects of flow inserts on heat transfer and critical heat flux," in *Proceedings of the 4th Int. Conference on Nuclear Engineering*, 10-13 March 1996, New Orleans, United State.

[11] D. J. Miller, F. B. Cheung, and S. M. Bajorek, "On the development of a grid-enhanced single-phase convective heat transfer correlation," *Nuclear Engineering and Design*, vol. 264, pp. 56–60, 2013, doi: 10.1016/j.nucengdes.2012.11.023.

[12] H.-Y. Gu, Z.-X. Hu, D. Liu, H.-B. Li, M. Zhao, and X. Cheng, "Experimental study on heat transfer to supercritical water in 2×2 rod bundle with wire wraps," *Experimental Thermal and Fluid Science*, vol. 70, pp. 17–28, 2016, doi: 10.1016/j.expthermflusci.2015.08.015.

[13] S. K. Yang and M. K. Chung, "Turbulent flow through spacer grids in rod bundles," *Journal of Fluids Engineering*, vol. 120, no. 4, pp. 786–791, 1998, doi: 10.1115/1.2820739.

[14] D. Caraghiaur, H. Anglart, and W. Frid, "Experimental investigation of turbulent flow through spacer grids in fuel rod bundles," *Nuclear Engineering and Design*, vol. 239, no. 10, pp. 2013–2021, 2009, doi: 10.1016/j.nucengdes.2009.05.029.

[15] H. Wang, Q. Bi, Z. Yang, W. Gang, and R. Hu, "Experimental and numerical study on the enhanced effect of spiral spacer to heat transfer of supercritical pressure water in vertical annular channels," *Applied Thermal Engineering*, vol. 48, pp. 436–445, 2012, doi: 10.1016/j.applthermaleng.2012.05.010.

[16] D. Palko and H. Anglart, "Theoretical and numerical study of heat transfer deterioration in high performance light water reactor," *Science and Technology of Nuclear Installations*, vol. 2008, p. 405072, 2008, doi: 10.1155/2008/405072.

[17] M. Jaromin and H. Anglart, "A numerical study of heat transfer to supercritical water flowing upward in vertical tubes under normal and deteriorated conditions," *Nuclear Engineering and Design*, vol. 264, pp. 61–70, 2013, doi: 10.1016/j.nucengdes.2012.10.028.

[18] H. Cheng, J. Zhao, and M. K. Rowinski, "Study on two wall temperature peaks of supercritical fluid mixed convective heat transfer in circular tubes," *International Journal of Heat and Mass Transfer*, vol. 113, pp. 257–267, 2017, doi: 10.1016/j.ijheatmasstransfer.2017.05.078.

[19] Y. Xiao, J. Li, J. Deng, X. Gao, H. Gu, and J. Pan, "Study of spacer effects on deteriorated heat transfer of supercritical fluid flow in an annulus," *Progress in Nuclear Energy*, vol. 123, p. 103306, 2020, doi: 10.1016/j.pnucene.2020.103306.

[20] S. Zhang, H. Gu, X. Cheng, and Z. Xiong, "Experimental study on heat transfer of supercritical Freon flowing upward in a circular tube," *Nuclear Engineering and Design*, vol. 280, pp. 305–315, 2014, doi: 10.1016/j.nucengdes.2014.09.017.

[21] C.-R. Zhao and P.-X. Jiang, "Experimental study of in-tube cooling heat transfer and pressure drop characteristics of R134a at supercritical pressures," *Experimental Thermal and Fluid Science*, vol. 35, no. 7, pp. 1293–1303, 2011, doi: 10.1016/j.expthermflusci.2011.04.017.

[22] C. Eze, K. W. Wong, T. Gschnaidtne, J. Cai, and J. Zhao, "Numerical study of effects of vortex generators on heat transfer deterioration of supercritical water upward flow," *International Journal of Heat and Mass Transfer*, vol. 137, pp. 489–505, 2019, doi: 10.1016/j.ijheatmasstransfer.2019.03.145.

[23] Z. Hu and H. Gu, "Heat transfer of supercritical water in annuli with spacers," *International Journal of Heat and Mass Transfer*, vol. 120, pp. 411–421, 2018, doi: 10.1016/j.ijheatmasstransfer.2017.12.056.

[24] K. Podila and Y. Rao, "Computational fluid dynamic simulations of heat transfer from a 2 × 2 wire-wrapped fuel rod bundle to supercritical pressure water," *Journal of Nuclear Engineering and Radiation Science*, vol. 4, no. 1, 2017, doi: 10.1115/1.4037747.

[25] K. Podila and Y. Rao, "CFD modelling of supercritical water flow and heat transfer in a 2×2 fuel rod bundle," *Nuclear Engineering and Design*, vol. 301, pp. 279–289, 2016, doi: 10.1016/j.nucengdes.2016.03.019.

[26] L. K. H. Leung, Y. Rao, and K. Podila, "Assessment of computational tools in support of heat-transfer correlation development for fuel assembly of canadian supercritical water-cooled reactor," *Journal of Nuclear Engineering and Radiation Science*, vol. 2, no. 1, 2015, doi: 10.1115/1.4031283.

[27] H. Wang, L. K. H. Leung, W. Wang, and Q. Bi, "A review on recent heat transfer studies to supercritical pressure water in channels," *Applied Thermal Engineering*, vol. 142, pp. 573–596, 2018, doi: 10.1016/j.applthermaleng.2018.07.007.

[28] Y. Wang *et al.*, "CFD simulation of flow and heat transfer characteristics in a 5×5 fuel rod bundles with spacer grids of advanced PWR," *Nuclear Engineering and Technology*, vol. 52, no. 7, pp. 1386–1395, 2020, doi: 10.1016/j.net.2019.12.012.

[29] X. Li, D. Chen, and L. Hu, "Numerical investigation on mixing performance in rod bundle with spacer grid based on anisotropic turbulent mixing model," *International Journal of Heat and Mass Transfer*, vol. 130, pp. 843–856, 2019, doi: 10.1016/j.ijheatmasstransfer.2018.10.121.

[30] H. Mao, B.-W. Yang, B. Han, and A. Liu, "Modeling of spacer grid mixing effects through mixing vane crossflow model in subchannel analysis," *Nuclear Engineering and Design*, vol. 320, pp. 141–152, 2017, doi: 10.1016/j.nucengdes.2017.05.003.

[31] B. Končar and S. Košmrlj, "Simulation of turbulent flow in MATIS-H rod bundle with split-type mixing vanes," *Nuclear Engineering and Design*, vol. 327, pp. 112–126, 2018, doi: 10.1016/j.nucengdes.2017.12.017.

[32] P. Zhao, T. Wan, Y. Jin, Z. Chen, Y. Li, and C. Peng, "Direct numerical simulation analysis of heat transfer deterioration of supercritical fluids in a vertical tube at a high ratio of heat flux to mass flowrate," *Physics of Fluids*, vol. 33, no. 5, p. 55114, 2021, doi: 10.1063/5.0046863.

[33] X. Chu and E. Laurien, "Direct numerical simulation of heated turbulent pipe flow at supercritical pressure," *Journal of Nuclear Engineering and Radiation Science*, vol. 2, no. 3, 2016, doi: 10.1115/1.4032479.